WATER IN THE FORMATION AND EARLY EVOLUTION OF MARS L.T. Elkins-Tanton and E. M. Parmentier[2], [1]MIT, Cambridge, MA, ltelkins@mit.edu, [2]Brown University, Providence RI, EM_Parmentier@brown.edu.

Introduction: The sources and destinations of water and carbon dioxide in terrestrial planet formation are poorly understood, but critical for the evolution of a planet. Though Martian surface morphology and composition shows the presence of liquid water during some period of evolution, the source of the water in planets is debated. The terrestrial planets almost certainly accreted from material that had some volatile content. Though the precise building blocks that made up the terrestrial planets are not agreed upon, significant volumes of volatiles can be found in both chondrites (up to 20%) and achondrites (up to 3%) [1, 2].

Early in accretion, the planetary embryo has a small gravitational field that adds relatively little acceleration to accreting material. Safronon and Vitjazev [3] estimate that up to a radius of about 1,300 km, a planetary embryo accretes material with sufficiently low energy that volatiles would be retained. Above this radius, heat of accretion devolatilizes newly accreting material. Assuming complete devolatilization above 1,300 km radius, a planet the size of Mars created entirely from material containing 0.5 wt% C and 1 wt% H_2O would obtain an initial silicate mantle with 0.01 wt% CO_2 and 0.06 wt% H_2O.

Several researchers have proposed that any water in the bulk accreting composition oxidized iron, allowing it to remain in the silicate mantle, while hydrogen was lost to space [4-6]. This model creates an entirely dry initial planet and requires later additions of water. Wänke and Dreibus [5] estimate that 36 ppm (0.0036 wt%) of water is left in the Martian mantle today, based on 100% degassing during accretion but eventual retention in a 130-m thick surface layer of oxidized material added at the very end of accretion (interestingly, this value is similar to those obtained in this paper for cumulates resulting from magma ocean solidification).

The balance between core formation and oxygen fugacity of accreting materials, however, is unknown. If accreting materials are relatively oxidized, then water will remain in the silicate portion of the planet to be partitioned during later differentiation processes. Processes of oxidation and hydrogen release may also be assumed to have reached equilibrium in the differentiated planetary embryos expected to produce the bulk of planetary accretion, and therefore the water contents of achondrites may be more pertinent than those of chondrites. The initial volatile contents used in these models may be thought of as those that remain following any oxidation of iron or partition of hydrogen into the core.

Models presented here demonstrate that clement surface conditions can be reached in less than 15 Ma after a planetary magma ocean, and that even small initial volatile contents can produce water-rich surfaces.

Methods and models: Though whole-mantle magma oceans remain possible but unproven [e.g. 7-10], there is a great likelihood that giant impactors late in accretion created giant magma ponds, which may then have evulsed onto the planetary surface, producing shallow planetary magma oceans [10,11]. These melting events may have been caused by the initial heat of accretion and early radiodecay, or they may have been produced by later giant impacts. Results presented here model either whole-mantle magma oceans or magma oceans 500 km in depth.

Volatiles are enriched in evolving magma ocean liquids as solid cumulates form and liquid volume decreases. Volatiles in excess of the saturation capacity of the magma will degas into the atmosphere when convection transports liquid close enough to the surface that bubbles can form and rise before being carried down again. As a limiting case, volatiles will partition between the atmosphere and the magma ocean liquids according to their equilibrium partial pressures. Both water and carbon dioxide can dissolve into silicate melts at quantities greater than 10 wt% at pressures above their degassing pressures [e.g. 12], though at a given pressure water will remain in silicate liquids in greater concentration than will carbon dioxide. Carbon dioxide and water saturation data are taken from Papale [12,13].

Heat flux and time scales

Magma ocean fluid dynamics are closely modeled by the dynamics of atmospheres, as noted by Solomatov [14]. Heat is transported from the interior to the surface by cold thermal plumes descending from the upper boundary layer, accompanied by more diffuse return flow of hotter material from the interior. Heat is transmitted conductively through the upper boundary layer into any existing early atmosphere, which in turn radiates this heat into space. This radiation is inhibited by the level of atmospheric emissivity, proceeding from the work of Priestley [15,16] and Abe and Matsui [17]. A solidification time scale can be calculated using heat flux F from the planet expressed as the following balance between total planetary heat flux on the left and the sum of latent heat of crystallization of

an increment of the magma ocean and secular cooling of an increment of the remaining magma ocean liquid:

$$4\pi R^2 F = \frac{dr}{dt}\rho H 4\pi r^2 + \frac{4}{3}\pi\rho C_p \frac{d}{dt}\left[T\left(R^3 - r^3\right)\right], \quad (1)$$

expressed in terms of planetary radius R, velocity of solidification front V, solid density ρ, heat of fusion H, radius of solidification r, heat capacity Cp, and change in solid temperature dT (dependent upon solidus slope). Temperature of the solid is assumed to remain at its solidus temperature on time scales of interest. Total heat flux F can be calculated as Stefan-Boltzmann radiation from the atmosphere

$$F = \varepsilon\sigma\left(T^4 - T_\infty^4\right), \quad (2)$$

where temperature is given in Kelvin, σ is the Stephan-Boltzmann constant, and emissivity ε is a function of optical depth τ*[18,19]:

$$\varepsilon = \frac{2}{\tau^* + 2}. \quad (3)$$

Emissivity is calculated separately for each atmospheric gas a function of the atmospheric partial pressure, as described in Abe and Matsui [17],

$$\tau^* = \left(\frac{3M_{atm}}{8\pi R^2}\right)\left(\frac{k_0 g}{3p_0}\right)^{\frac{1}{2}} \quad (4)$$

where M_{atm} is the mass of the specific atmospheric gas, R is the planetary radius, and k_0 is the atmospheric absorption coefficient of a specific gas at pressure p_0. [The mass of a gas in the atmosphere can be calculated from equations using the relation $M_{atm} = (4\pi p_x R^2/g)$.]

The atmosphere is treated as a grey radiative emitter with no convective heat transport. If the atmosphere were modeled as convective, which it may be in these models given its densities and temperatures, cooling would occur faster and the effective radiative transfer level moved well above the planet's surface. No speciation in the atmosphere is calculated, and all degassed material is assumed to stay in the atmosphere. No atmospheric stripping or hydrodynamic escape occurs in these models, and no gravitationally bound atmosphere is assumed to exist before the magma ocean stage. These models thus should be treated as a simple end-members.

Magma solidifies into a cumulate mantle

Both the Martian and terrestrial magma oceans are expected to crystallize perovskite and magnesiowustite at pressures higher than 22 GPa, majorite and ringwoodite between 20 and 15 GPa, garnet, orthopyroxene, clinopyroxene, and olivine between 14 and 3 GPa, with spinel replacing garnet between 3 and 1 GPa, and plagioclase replacing spinel between 1 GPa and the surface. At pressures and temperatures of magma ocean crystallization no hydrous or carbonate minerals will crystallize [20,21]. Nominally anhydrous minerals can contain a dynamically and petrologically significant amount of OH [22-26] (as much as 1000 ppm, and with contributions from minimal interstitial liquids, resulting mantle solids can retain 0.25 to 0.5 wt% H2O). Carbon dioxide, in contrast, cannot partition into mantle minerals in as significant quantities [27].

The magma ocean is assumed to solidify from the bottom upward, because the steep slope of the adiabat first intersects the shallower slope of the solidus at depth. Solids are assumed to retain their solidus temperatures during solidification because the speed of solidification is fast compared to thermal diffusion. The solidus used for Mars is fitted to data from Longhi *et al.* [28].

Surface temperature is calculated by following the adiabat upward from the top of the fully-solidified cumulate layer. The adiabat must be moved to lower temperatures to account for latent heat of crystallization when lying in regions between the solidus and liquidus; we assume that latent heat is distributed linearly between solidus and liquidus.

This one-dimensional model calculates atmospheric composition and mass, magma ocean liquid mass and composition, and composition and density of fractionating cumulate mantle phases in small increments from the point that the magma ocean is entirely liquid to its final increment of solidification. Mineral compositions are calculated in equilibrium with the magma ocean composition using experimental distribution coefficients as described in [29]. Elkins-Tanton et al. [29] also describes the thermophysical parameters and techniques used to calculate each mineral's density by temperature, pressure, and composition. Trace element partitioning is described in Elkins-Tanton et al. [30, 31]. Subsequent cooling is calculated solving the transient heat conduction equation in a spherical geometry using the temperature distribution that results from overturn along with heat flux from the planetary surface through the final atmospheric mass.

Results: Magma ocean solidification and subsequent planetary evolution proceeds through three major phases, shown in Figure 1. First, the magma ocean solidifies, partitioning volatiles between solid cumulates, evolving liquids, and a growing primordial atmosphere. In these simplified models the timescale of solidification is limited by the emissivity of the atmosphere. This step produces cumulates unstable to overturn and carrying a small water budget available for release in later volcanism, and it produces a significant surface volatile reservoir in the atmosphere.

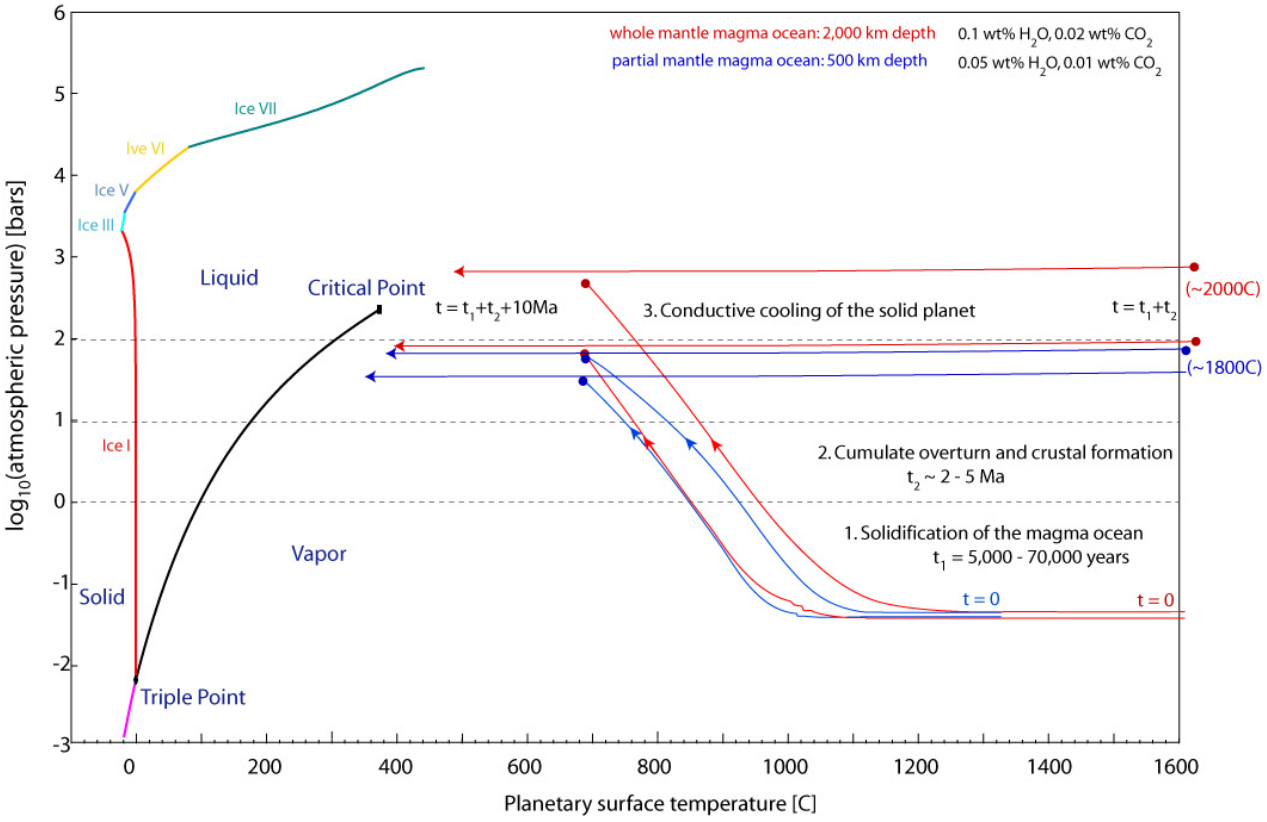

Figure 1: Cooling paths for planetary solidification and subsequent conductive cooling plotted on a water phase diagram (after http://www.chemicalogic.com/download/phase_diagram.html). Two whole-mantle magma oceans (red) and two 500-km magma oceans (blue) with differing initial volatile contents are shown. During solidification the atmosphere grows while the planet cools (stage 1). Cumulate overturn (not shown) raises the surface temperature again as hot cumulates rise, and then cooling resumes as heat is conducted from the interior through the existing atmosphere (stage 3). Surface temperatures approach the water liquid-vapor critical point within about 15 Ma after magma ocean formationm regardless of magma ocean depth. With atmospheric loss cooling paths may drop below the critical point and enter the liquid water region through the liquid-vapor phase boundary, but with higher initial volatile contents the atmospheric pressures can rise significantly, again placing conditions in the supercritical region.

Solidification rates limited by radiative heat loss through the atmosphere may be very fast, with 90% by volume of the magma ocean solidifying in as little as 10,000 years (Fig. 1). In further models including convective heat transfer through the atmosphere and atmospheric loss, cooling may proceed even faster. Even the rates predicted in these models probably allow almost complete solidification before solid-state gravitationally-driven cu-mulate overturn.

The atmospheres produced in these models exclusively through degassing of the small initial volatile contents are significant. A whole-mantle magma ocean beginning with 0.05 wt% of water and 0.01 wt% of carbon dioxide produces an atmosphere of 170 bars. Though Mars is relatively dry today, as much as 99% of Mars' original volatiles are thought to have been lost by 3.8 GPa through escape through impacts, sputtering by solar wind, and hydrodynamic escape [32]. The high initial atmospheric masses predicted here are consistent with these models.

Though the great majority of volatiles remain in the evolving liquids or are degassed into the atmosphere, a geodynamically significant quantity is sequestered in the solid cumulates, as much as 0.05 wt% OH in even the driest models, without considering interstitial liquids (Figure 2). In the absence of plate tectonics, therefore, mantle volatile content should be controlled by magma ocean processes. Initial mantle water content should have a significant effect on creep rates and thus mantle viscosity and onset and vigor of any subsequent solid-state mantle convection.

The second major and probably unavoidable phase of evolution begins near or at the end of solidification when the solidified cumulates overturn gravitationally to a stable density profile (2. in Figure 1). During overturn hot cumulates rise from depth and melt adia-

batically to produce the earliest crust. Because the cumulates carry a small but non-negligible volatile budget and magma will partially degas as it erupts, overturn produces an addition to the atmosphere. More importantly, perhaps, the significant atmospheric pressure allows erupting lavas to retain some volatile content as they solidify. Under 100 bars pressure lava can retain 1 wt% water. These models predict that the earliest basaltic crusts will have variable water content (depending upon the com-position of the source and the extent of melting) up to about 1 wt%. The eruption of this magma also releases a pulse of heat into the atmosphere from the heat of fusion during crystallization. Numerical models indicate that the major phase of overturn is complete in 2 to 3 million years, far longer than solidification but still geologically rapid.

The final stage in these models is cooling of the solidified, stable planet (3. in Figure 1). This cooling proceeds entirely by conduction to the planetary surface and, in these models, radiation through the atmosphere. The compositionally stable cumulate mantle resists the onset of thermal convection long past the endpoints of these models [33], making conductive cooling a reasonable approximation. Taking the final temperature profile of the overturned mantle and allowing conduction to proceed, cooling of the planetary surfaces follows paths that pass close to the water critical point after about 10 Ma, implying the presence of supercritical fluids on early planetary surfaces.

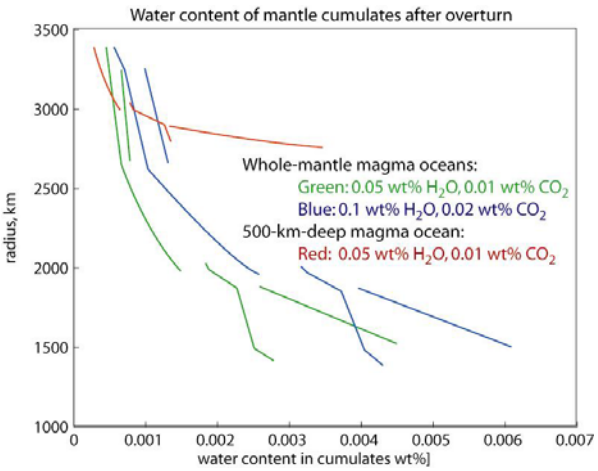

Figure 2: Water contents of cumulate mantle following overturn to gravitational stability. Where two compositions are indicated at a single level, the mantle is laterally heterogeneous. Water contents approach nominally-dry terrestrial mantle values.

Conclusions: These models indicate that with small initial volatile contents partial-mantle magma oceans can produce significant atmospheres. Even without convective heat transfer and without allowing for any atmospheric loss, the entire process of solidification, overturn, and cooling to clement conditions is likely to occur within 15 - 20 Ma. This short interval indicates that serial magma oceans of varying depths were probably unavoidable on the early terrestrial planets, up through the Late Heavy Bombardment. These time estimates are reasonable for volatile-bearing planets of Martian or greater size; smaller, drier bodies such as the Moon likely produced anorthite flotation crusts, significantly slowingcooling and their solidification.

Degassing produces a water-rich initial atmosphere that will partially escape and partially condense and provide surface water. The earliest crust also contains some volatile content. The terrestrial planets therefore may have had clement surface conditions and a basaltic crust within15 to 20 Ma of accretion, and in a similar interval after any subsequent giant impact.

References: [1] Wood (2005) Chondrites and the Protoplanetary Disk, ASP Conference Series V. 341. [2] Jarosewich (1990) Meteoritics 25, 323-337. [3] Safronov, Vitjazev (1986) Chemistry and Physics of Terrestrial Planets, Springer-Verlag. [4] Ringwood (1979) On the Origin of the Earth and Moon. Springer Verlag. [5] Wänke, Dreibus (1994) Phil. Trans. Royal Soc. London A 359, 285-293. [6] Hunten *et al.* (1987) Icarus 69, 532-549. [7] Wood *et al.* (1970) Proc. Apollo 11 LPSC, 965-988. [8] Smith *et al.* (1970) Proc. Apollo 11 LPSC, 897-925. [9] Warren (1985) *Ann. Rev. Earth Planet. Sci. 13*, 201-240. [10] Tonks and Melosh (1993) *JGR 98*, 5319-5333. [11] Reese C.C. and V.S. Solomatov (2007) Icarus. [12] Papale (1999) Am. Min. 84, 477-492. [13] Papale (1997) CMP 126(3), 237-251. [14] Solomatov (2000) Origin of the Earth and Moon, U. Arizona Press. [15] Priestley (1959) Turbulent Transfer in Lower Atmosphere, U. Chicago Press. [16] Priestley (1957) Proc. R. Soc. London A238, 287. [17] Abe and Matsui (1988) J. Atm. Sci. 45 (21), 3081-3101. [18] Pujol, North (2003) Tellus Ser. A., 55 (4), 328-337. [19] Hodges (2002) GRL 29 (3), Art. No. 1038. [20] Ohtani *et al.* (2004) PEPI 143-144, 255-269. [21] Wyllie and Ryabchikov (2000) J. Pet. 41, 1195-1206. [22] Koga, *et al.* (2003) G^3 4(2), doi 10.1029/2002GC000378. [23] Aubaud *et al.* (2004) GRL 31, doi:10.1029/2004GL021341. [24] Forneris, and Holloway (2003) EPSL 214, 187-201. [25] Bell *et al.* (2004) J. Pet. 45, 1539-1564. [26] Bolfan-Casanova and Keppler (2000) EPSL 182, 209-221. [27] Keppler *et al.* (2003) Nature 424, 414-416. [28] Longhi *et al.* (1992) Mars, U. Arizona Press. [29] Elkins-Tanton *et al.* (2003) MAPS 38, 1753-1771. [30] Elkins-Tanton *et al.* (2005) EPSL 236, 1-12. [31] Elkins-Tanton *et al.* (2005) JGR 110, doi:10.1029/2005JE002480. [32] Catling (2004) Ency. Paleoclimatology and Ancient Environments. [33] Zaranek and Parmentier (2004) JGR, doi: 10.1029/2003JB002462.